

## Effect of silver nitrate ( $\text{AgNO}_3$ ) on the growth, optical, spectral, thermal and mechanical properties of $\gamma$ -glycine single crystal

C. SEKAR\*, R. PARIMALADEVI

*Department of Physics, Periyar University, Salem – 636 011, Tamilnadu, India*

Single crystal of  $\text{AgNO}_3$  doped  $\gamma$ -glycine, a nonlinear optical (NLO) material have been grown by slow evaporation method. The phase purity and crystal structure of the grown crystals have been confirmed by powder X-ray diffraction studies. Thermal analysis was carried out to study the effect of  $\text{AgNO}_3$  doping on thermal stability of  $\gamma$ -glycine crystal. Functional groups of the grown crystal were identified through FTIR and FT-Raman spectroscopy. The optical transparency and lower cut off value of UV transmission were ascertained by recorded UV- Visible spectrum of  $\gamma$ -glycine crystals. The existence of second harmonic generation (SHG) of the grown crystal was confirmed by Kurtz-powder technique and the efficiency of frequency doubling was found to be 1.4 times than that of KDP. Mechanical property of the grown  $\text{AgNO}_3$  doped  $\gamma$ -glycine crystal was studied by Vickers microhardness tester.

(Received March 29, 2009; accepted May 28, 2009)

*Keywords:* Nonlinear optical materials;  $\gamma$ -glycine; Growth from solution; Vibrational spectroscopy; Thermal properties

### 1. Introduction

The search for non-linear optical (NLO) material has been of great interest in recent years due to their widespread applications such as high-speed information processing, optical communications and optical data storage [1]. Within the last decade much progress has been made in the development of these NLO organic materials having large nonlinear optical coefficients. One of the advantages in working with organic materials is that they allow one to fine-tune the chemical structures and properties for the desired nonlinear optical properties. In addition, the organic crystals have large optical susceptibility, inherent ultra fast response times and high optical threshold for laser power as compared with inorganic materials. Moreover, their lower cut off wavelength and a wide transparency window in the visible region makes the candidate materials subject for extensive investigation [2]. Aminoacids are interesting materials for NLO application as they contain proton donar carboxyl acid (-COO) group and the proton acceptor amino ( $\text{NH}_2$ ) group in them [3]. Especially some aminoacids like arginine, lysine, l-alanine and  $\gamma$ -glycine are evidently showing NLO activity because they have a donar  $\text{NH}_2$  group and acceptor COOH group and also intermediate charge transfer was possible.

Glycine, the simplest aminoacid, has three polymeric crystalline forms:  $\alpha$ ,  $\beta$  and  $\gamma$ . Both  $\alpha$  and  $\beta$  forms crystallize in centrosymmetric space group  $\text{P}2_1/c$ .  $\gamma$ -glycine crystallizes in non-centrosymmetric space group  $\text{P}3_1$  making it a candidate for piezo-electric and NLO applications [4, 5]. The metastable  $\alpha$ -glycine grown from aqueous solution transforms into  $\gamma$ -form spontaneously. The least stable  $\beta$ -form is always obtained from water-alcohol mixed solvent. The  $\beta$ - form transforms rapidly to  $\alpha$ - and  $\gamma$ - forms in presence of moisture at room temperature. The more stable  $\gamma$ -glycine crystals are grown from aqueous solution or gel in the presence of additives. The  $\gamma$ -form transforms to  $\alpha$  form on heating around  $170^\circ\text{C}$  [6]. Narayan Bhat et.al [6] reported that the morphology of the glycine crystals grown from various solvents such as sodium hydroxide, sodium fluoride, sodium nitrate and sodium acetate showed a marked difference in transition temperature and second harmonic conversion (SHG) efficiency. The SHG efficiency of  $\gamma$ -glycine

grown in presence of NaF, NaOH and NaCH<sub>2</sub>COOH were reported to be 1.3, 1.4 and 1.2 times higher than that of potassium dihydrogen phosphate (KDP) crystal. The same authors have reported that the  $\gamma$ -crystal grown from a mixture of glycine and NaOH undergoes a transition from  $\gamma$  to  $\alpha$  form at 172°C. Choudary et.al [7] has studied the low temperature ferroelectric phase transition of glycine silver nitrate (GSN) single crystals. Since silver nitrate crystal can crystallize in non-centrosymmetric space group and it has high transmission range, in present work, we choose silver nitrate as dopant and studied the optical property of AgNO<sub>3</sub> doped  $\gamma$ -glycine crystals for the first time.

## 2. Experimental

The  $\alpha$ -glycine was crystallized by taking the analar grade 1M glycine (99%). In another series  $\gamma$ -glycine was synthesized by taking 1M glycine with two different concentration of silver nitrate (0.1 and 0.2M). Impurity content in glycine and  $\gamma$ -glycine was minimized by successive recrystallization process. The pH value of the saturated glycine solution was found to be 4. In case of AgNO<sub>3</sub> added glycine solution, the pH values increased with increase in silver nitrate concentrations; 4.80 and 5.34 for 0.1 and 0.2 M respectively. As the growth rate of a crystal depends on solubility and growth temperature, the solubility of glycine and  $\gamma$ -glycine synthesized in presence of various concentration of AgNO<sub>3</sub> in double distilled water were determined at various temperatures [Fig.1]. It can be seen that the solubility of  $\alpha$ -glycine was higher than that of  $\gamma$ -glycine. Moreover, the solubility increases with increase in temperature and decreases with increase in concentration of AgNO<sub>3</sub>. This result confirms that the  $\gamma$ -glycine grown in presence of AgNO<sub>3</sub> was stable and less water soluble than glycine at room temperature. In both cases, positive slope of the solubility curve enables growth by slow evaporation method. The final solution was filtered using 0.1 micron porosity filter papers and kept in beakers covered with perforated sheets. The spontaneous evaporation of the solvent at room temperature yielded crystals in the time span of 15-20 days. The grown crystals were carefully harvested and then subjected to characterization studies.

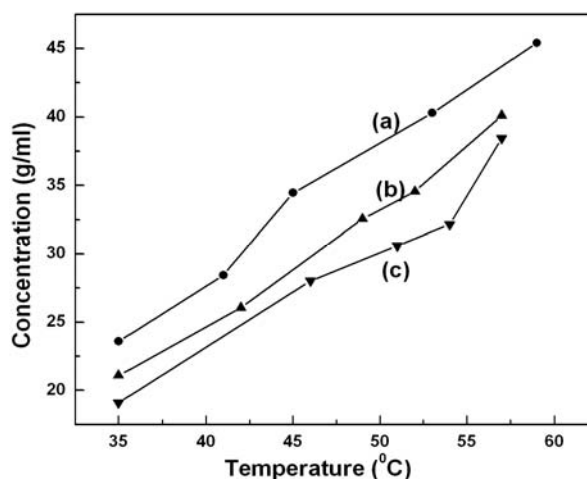


Fig.1. Solubility curves of glycine (a) without and with incorporation of AgNO<sub>3</sub> (b) 0.1M (c) 0.2M.

Glycine crystals grown with silver nitrate were powdered and mixed with KBr pellets for obtaining transmission spectra in the mid IR region (4000-400cm<sup>-1</sup>) using Perkin Elmer (Spectrum RX1) and FT Raman spectra was recorded using NEXUS670. Powder XRD pattern was recorded on Bruker diffractometer within the 2 $\theta$  range of 10 to 80° using CuK $\alpha$  as X-ray source ( $\lambda = 1.5406\text{\AA}$ ) to confirm crystal quality and to identify the cell parameters. Thermogravimetry of samples was performed using TA instruments SDT Q600 V8.3. UV - Visible spectrum was

recorded on a PerkinElmer Lambda 25 spectrometer in transmission mode. Second harmonic generation efficiency of the samples was determined using Kurtz powder method. A Q switched Nd:YAG laser beam of wavelength 1064nm was used with an input energy of 1.35MJ/pulse and pulse width of 8ns, the repetition rate being 10Hz. The SHG radiations of 532 nm (green light) emitted were collected by a photo multiplier tube (PMT- Philips photonics model 8563) and the optical signal incident on the PMT was converted into voltage output at the CRO (Tektronix –TDS 3052B). Microhardness measurements were carried out on the grown crystals using Shimadzu tester.

### 3. Results and discussion

#### 3.1 Crystal growth

Figs. 2 & 3 show the crystal habits of  $\gamma$ - glycine grown in presence of  $\text{AgNO}_3$  (0.1M and 0.2M) respectively. The crystals grown in presence of lower concentration of  $\text{AgNO}_3$  (0.1M) shows prismatic shape as like  $\alpha$ -glycine with comparatively long growth along the 'c' direction than 'a' as reported by Dawson et.al [8]. Morphology of the 0.2M  $\text{AgNO}_3$  doped crystals changed significantly when compared to that of pure glycine. When the crystal face has a structure similar to that of a face of the crystal of the adsorbed substance a particle of the latter will adhere to the crystal face just as it would happen with the corresponding face of its own crystal, since it experiences similar forces. Thus, on the growing face, impurity particles are strongly adsorbed together with particles of the main substances [9]. Upon further increase in concentration, silver nitrate affects the growth rate of the crystal faces through incorporation into the lattice, disturbing crystal arrangement. Further  $\text{AgNO}_3$  incorporation promotes the growth along 'a' direction and reduces the growth along 'c'. Thus the crystal morphology of glycine crystal grown in the presence of 0.2M of  $\text{AgNO}_3$  changed to bipyramids. Also, there is a significant change in the color of the crystal due to the silver nitrate doping i.e.,  $\gamma$ -glycine grown in presence of  $\text{AgNO}_3$  was brown in color. In both the cases, the crystals were transparent.



Fig. 2. As grown 0.1 M  $\text{AgNO}_3$  doped  $\gamma$ -glycine crystal.

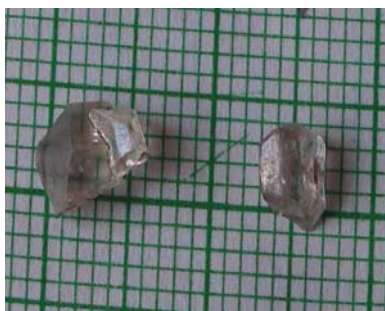


Fig. 3. As grown 0.2 M  $\text{AgNO}_3$  doped  $\gamma$ -glycine crystal

### 3.2. X-Ray diffraction analysis

The crystal structure of glycine was reported by Dawson et.al [8]. The  $\gamma$ -glycine crystallizes in hexagonal structure with space groups of  $P3_1$ . X-ray powder diffraction patterns of the grown crystals were shown in Fig. 4. The results agree well with the simulated XRD pattern of pure  $\gamma$ -glycine and the characteristic peaks have appeared at around  $25.3^\circ$  ( $2\theta$ ). Slight shift in the peak position may be due to doping of  $\text{AgNO}_3$  in  $\gamma$ -glycine crystal. Appearance of sharp and strong peaks confirms the good crystallinity of the grown samples. The estimated lattice parameters of  $\gamma$ -glycine grown with incorporation of various concentration of  $\text{AgNO}_3$  were given in Table 1.

Table1. Lattice parameters of  $\gamma$ -glycine grown with various concentration of  $\text{AgNO}_3$ .

AgNO <sub>3</sub> concentration selected for growing $\gamma$ - glycine	Lattice parameters	
	a = b (Å)	c (Å)
0.0M <sup>a</sup>	6.86	5.43
0.1M <sup>b</sup>	6.88(1)	5.40(2)
0.2M <sup>b</sup>	7.04(1)	5.36(1)

a, Dawson et.al [8]; b, present work

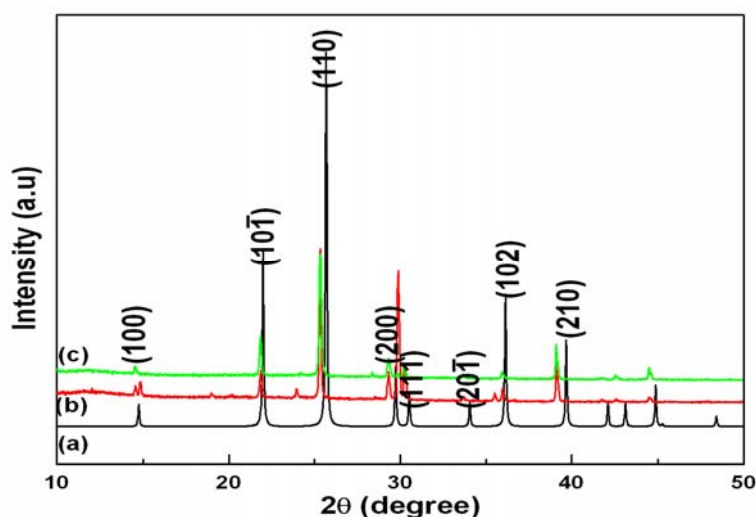


Fig.4. (a) Calculated XRD pattern of  $\gamma$ -glycine and experimental powder XRD pattern of  $\gamma$ -glycine grown in presence of (b) 0.1M (c) 0.2M of  $\text{AgNO}_3$

### 3.3 Thermal analysis

Figs.5 and 6 illustrate the TG-DTA curves of 0.1M and 0.2M  $\text{AgNO}_3$  doped  $\gamma$ -glycine crystals respectively. The experiments were performed in the temperature range of  $20^\circ$ - $1100^\circ\text{C}$  in

nitrogen atmosphere with the heating rate of  $20^\circ\text{C}/\text{min}$ . The TGA curves show no change in weight before  $215^\circ\text{C}$  for both the samples, which eliminate the possibility of hydrate or solvate incorporation into crystals. The major weight loss ( $\sim 35\%$ ) occurred in the temperature range between  $230\text{--}300^\circ\text{C}$  which could be attributed to the sublimation and decomposition of glycine resulting in the release of  $\text{NH}_3$  and  $\text{CO}$  molecules. This decomposition was indicated by the endothermic peak near  $265^\circ\text{C}$  in DTA curve. Appearance of an endothermic peak at  $170^\circ\text{C}$  in DTA curve of  $0.1\text{M}$   $\text{AgNO}_3$  doped  $\gamma$ -glycine corresponds to the transformation of  $\gamma$ - to  $\alpha$ -phase. This transition temperature got increased to  $208^\circ\text{C}$  for the doped crystal ( $0.2\text{M}$   $\text{AgNO}_3$ ). Note that there is no change in mass corresponding to the transition temperature in both cases which indicates that the observed DTA peaks are related to structural phase transition only. The observed increase in phase transition temperature is much higher than the value reported for  $\gamma$ -glycine crystals grown from a mixture of different solvents [6, 10, 11]. This improvement in transition temperature could be attributed to the  $\text{AgNO}_3$  doping into  $\gamma$ -glycine which makes the crystal closely packed. The DTA curve of  $0.2\text{M}$   $\text{AgNO}_3$  doped  $\gamma$ -glycine reveals no endothermic/exothermic peak below  $208^\circ\text{C}$  suggesting its structure stability in the temperature range. This ensures the suitability of the material for possible application in laser, where the crystal is required to withstand high temperature.

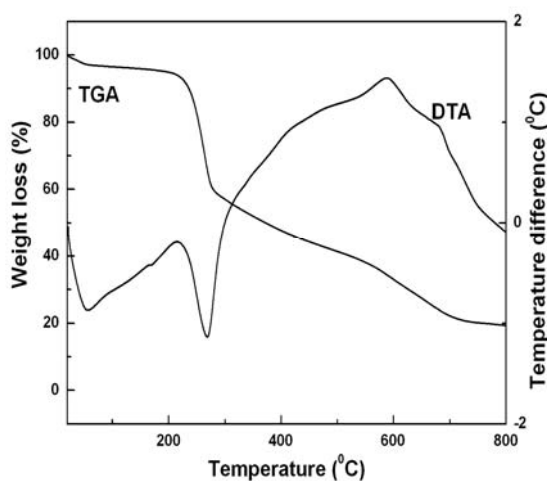


Fig.5. TG-DTA curve  $\text{AgNO}_3$  ( $0.1\text{M}$ ) doped  $\gamma$ -glycine crystal.

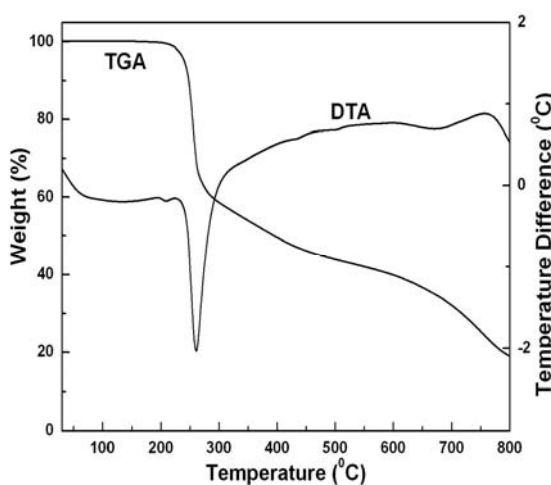


Fig. 6. TG-DTA curve of  $\text{AgNO}_3$  ( $0.2\text{M}$ ) doped  $\gamma$ -glycine crystal.

### 3.4 FTIR and FT-Raman analyses

The FTIR and FT-Raman spectra of powdered glycine grown with  $\text{AgNO}_3$  were shown in the Figs. 7 & 8 respectively. Though  $\text{AgNO}_3$  concentration in the grown crystals was not

quantitatively measured it was indirectly studied by these spectral analyses. The observed wave numbers, relative intensities obtained from the recorded spectra and the assignments proposed for both crystals were found to be in good agreement with the assignment proposed in reported literature [12, 13] and are listed in Table 2. In FTIR spectra broad envelope in the higher wavenumber region between 3700- 2100  $\text{cm}^{-1}$  was due to hydrogen interaction with other atoms such as N-H stretching of  $\text{NH}_2$  and C-H of  $\text{CH}_2$  stretching. The broad nature of this region became narrow in 0.2M  $\text{AgNO}_3$  doped crystals. The peak observed at 2989 $\text{cm}^{-1}$  in Raman spectra was due to C-H stretching. Two overlapped bands at around 1612  $\text{cm}^{-1}$  and 1404  $\text{cm}^{-1}$  in FTIR spectra were attributed to the asymmetric and symmetric stretch mode of the  $\text{COO}^-$  group. While increasing dopant (0.2M) concentration this peak was shifted to 1634  $\text{cm}^{-1}$  and 1399  $\text{cm}^{-1}$  respectively. Other bands of  $\text{COO}^-$  deformation mode were observed at 690 and 502  $\text{cm}^{-1}$ . These bands were seen at 687 and 506  $\text{cm}^{-1}$  in the Raman spectra. Both the results confirmed that the glycine molecule existed in zwitterions form inside the crystal. This caused an antiparallel arrangement, which contributed to non-centrosymmetric crystalline growth. Choudary et.al [7] reported that silver ion bridge the centrosymmetrically related carboxyl groups ( $\text{COO}^-$ ) to form dimers. The medium intensity peak at 1033  $\text{cm}^{-1}$  related to C-C-N asymmetric stretching became weak and got shifted to 1049  $\text{cm}^{-1}$  in the doped GG crystal. The characteristics peak of GG crystal observed at 927  $\text{cm}^{-1}$  for 0.1M  $\text{AgNO}_3$  doped crystal got shifted to 905  $\text{cm}^{-1}$  for 0.2M doped GG crystal. In Raman spectra vibration due to CCN stretching observed at 387 and 319  $\text{cm}^{-1}$  for 0.1M doped crystal got shifted to 341 and 309  $\text{cm}^{-1}$  for 0.2M doped crystal which confirmed the  $\text{AgNO}_3$  doping into the target compound.

In Raman spectra there was a significant increase in peak intensities of the 0.2M  $\text{AgNO}_3$  doped crystal when compared to that of 0.1M doped crystal. In addition major shifts with known frequency and additional peaks corresponding to the internal modes in the mid region have been observed in this study. This recommends that the  $\text{AgNO}_3$  was doped into  $\gamma$ -glycine crystal and the when the dopant concentration in crystal with its increases in starting supersaturated solution.

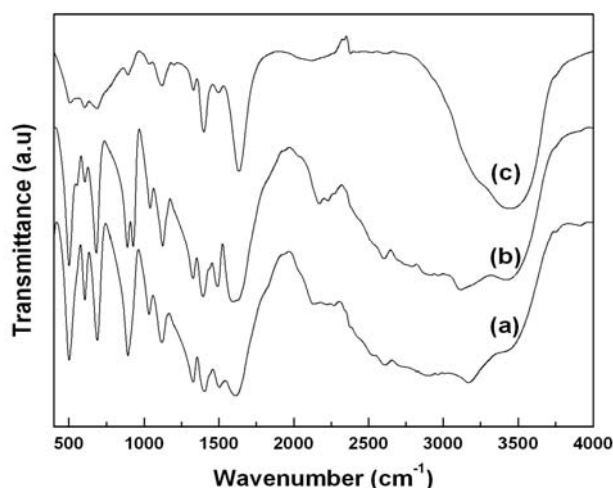


Fig.7. FTIR spectra of (a)  $\alpha$ - glycine and  $\gamma$  - glycine crystal grown in presence of (b) 0.1M (c) 0.2M of  $\text{AgNO}_3$ .

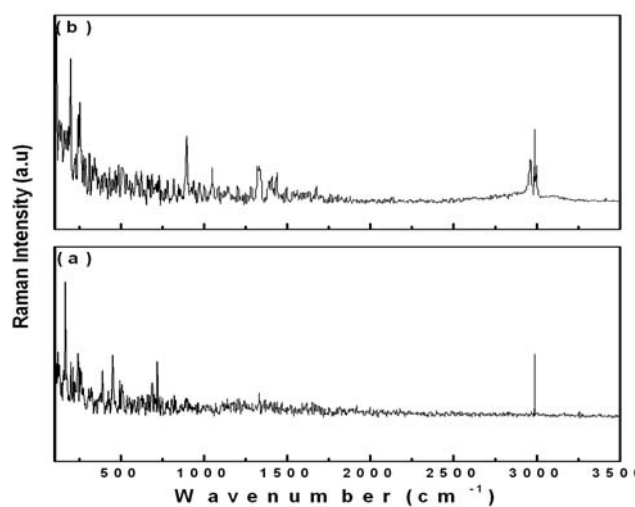


Fig.8. FT-Raman spectra of  $\gamma$ -glycine crystal grown in presence of (a) 0.1M (b) 0.2M of AgNO<sub>3</sub>

Table 2. Observed IR and Raman wavenumbers (cm<sup>-1</sup>) of  $\alpha$ - glycine and  $\gamma$  - glycine grown in presence AgNO<sub>3</sub>

$\alpha$ - glycine FTIR	$\gamma$ - glycine grown in presence of 0.1M AgNO <sub>3</sub>		$\gamma$ - glycine grown in presence of 0.2M AgNO <sub>3</sub>		Tentative assignment
	FTIR Raman	FT- Raman	FTIR Raman	FT- Raman	
<b>3908w</b>					
<b>3171s</b>	3422s		3433s		$\nu_{as}(\text{NH}_3)^+$
<b>2899m</b>	3119s				$\nu_s(\text{NH}_3)^+$
	2989m		2989m		$\nu_{as}(\text{C-H})$
<b>2612m</b>	2792m		2963w		$\nu_s(\text{C-H})$
<b>2270m</b>	2604m				
<b>2135w</b>	2228w		2617w		
<b>1612vs</b>	2172w		2381w		
<b>1502s</b>	1597vs		2121w		
	1492s		1634m		$\nu(\text{N-H-O})$
<b>1404s</b>			1498w		
<b>1328s</b>	1394s				
<b>1119m</b>	1327s		1438w		
<b>1033m</b>	1331w		1399m		$\nu_{as}(\text{COO}^-)$
	1125m		1330w		
	1041w		1322w		$\delta(\text{NH}_3)$
<b>892m</b>	927 m		1119w		$\delta(\text{CH}_2)$
<b>690m</b>			-		
<b>607w</b>			905w		$\nu_s(\text{COO}^-)$
			892w		
	888 m				$\omega(\text{CH}_2)$

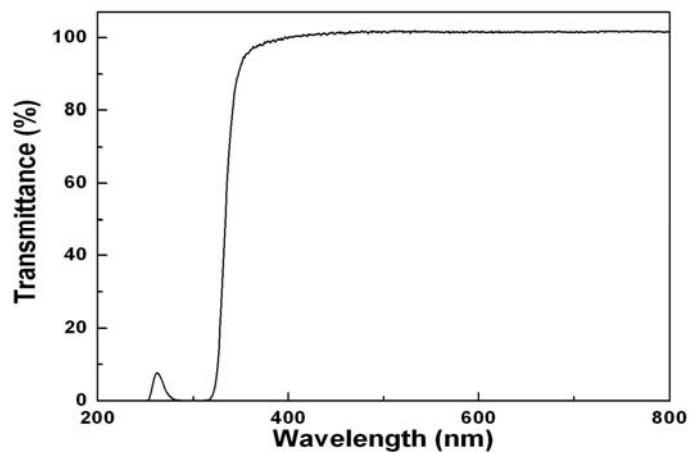
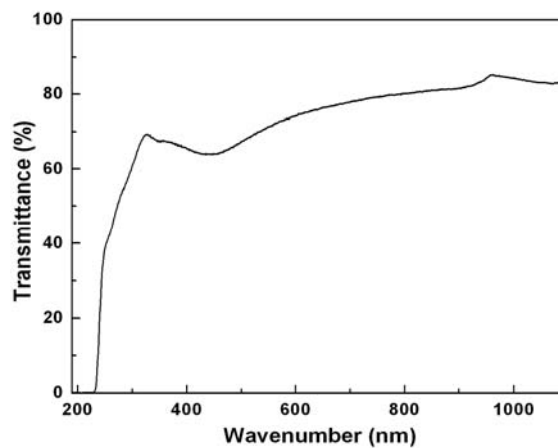
<b>502m</b>			687w	
	718m		686w	$\rho$ ( $\text{NH}_3$ )
			607w	$\nu_{\text{as}}$ (CCN)
		684m	621w	characteristic peak of GG
	687w		592w	
		607w	509w	
			506w	$\nu_{\text{s}}$ (CCN)
		502m		-
	506w		485w	$\delta$ ( $\text{COO}^-$ )
				$\omega$ ( $\text{COO}^-$ )
	492w		450w	
				$\rho$ ( $\text{COO}^-$ )
	450m		428w	
				$\rho$ ( $\text{COO}^-$ )
	423w		341w	
387m		309w		
			285-	
319w		127	$\delta$ (CCN)	
	252-		$\delta$ (CCN)	
119		109vs	Lattice modes	
101m			$\tau$ (C-C)	

$\nu$ , stretching;  $\rho$ , rocking;  $\delta$ , deformation;  $\omega$ , wagging,  $\tau$ , torsion; w, weak; m, medium, s, strong, vs, very strong.

### 3.5 Optical transmission spectral analysis

Good optical transmittance and lower cut off wavelengths are very important properties for NLO crystals. In these crystals the UV- Visible range from 200 to 400 nm is very important for the realization of SHG output in this range using diode and solid-state lasers. The UV transmission spectrum of  $\gamma$ - glycine and  $\text{AgNO}_3$  doped  $\gamma$ -glycine is shown in Figs.9 & 10. It can be seen from the transmission curve that the lower cutoff wavelength lies nearly 320 and 230 nm for  $\gamma$ -glycine and  $\text{AgNO}_3$  doped  $\gamma$ -glycine crystals make potential material for frequency doubling. Thus lower cut off value changed from near UV region (320nm) to middle UV region (230nm) may due to  $\text{AgNO}_3$  doping. The absence of absorption in the visible region clearly indicates that the grown crystal can be used for optoelectronic application. High transmittance % is observed from 500nm which clearly indicates the crystal possess good optical transparency for SHG of Nd:YAG laser.



Fig. 9. UV- Visible spectra of  $\gamma$ -glycine.Fig.10. UV- Visible spectra of  $\text{AgNO}_3$  doped  $\gamma$ -glycine.

### 3.6 Powder SHG measurement

In order to confirm the NLO property, the grown crystals were powdered and subjected to Kurtz and Perry powder technique, which remains powerful tool for initial screening of materials for SHG [14]. The second harmonic signal generated in the crystalline sample was confirmed from the emission of green radiation ( $\lambda = 534\text{nm}$ ) from the crystal. The measured amplitude of second harmonic green light for  $\text{AgNO}_3$  doped  $\gamma$ -glycine is 135mV against 95mV for KDP crystal. The result obtained shows a powder SHG efficiency of  $\text{AgNO}_3$  doped  $\gamma$ -glycine is about 1.4 times that of potassium dihydrogen orthophosphate. This may be due to central ion in metal organic complex offers a certain anisotropic field to keep NLO active chromophores which drastically vary the hyperpolarizability value [15].

### 3.7 Vickers Microhardness Studies

Hardness is a measure of materials' resistance to localized plastic deformation. It plays key role in device fabrication. The mechanical property of  $\gamma$ -glycine and  $\text{AgNO}_3$  doped  $\gamma$ -glycine crystals was studied by Vickers hardness test. The applied loads were 25, 50, 100 and 200 grams. The measurement was done at different points on the crystal surface and the average value was taken as the Hv for a given load.

The micro hardness was calculated using the relation

$H_v = 1.8544 P/d^2$  ( $\text{kg/mm}^2$ ) where  $P$  is the applied load and  $d$  is the diagonal length of the indentation impression.

The calculated Vickers hardness values for pure and  $\text{AgNO}_3$  doped  $\gamma$ -glycine crystals as a function of load was shown in Fig.11 Vickers Hardness values of doped crystals are higher than that of pure sample. It can be noticed that the doped crystal has higher  $H_v$  value ( $38 \text{ kg/mm}^2$ ) than that of pure crystal ( $10 \text{ kg/mm}^2$ ). The hardness values of both pure and doped crystals increase with increasing load. The reverse indentation size effect involves increase in hardness value with increasing load [16]. In the doped crystal a crack developed on the surface upon applying the load of 200g where as the undoped crystal broke at 100g itself. This was attributed to the incorporation of the  $\text{AgNO}_3$  into glycine crystals, which make the doped crystal closely packed than the pure crystal [17]. This result confirmed that the  $\text{AgNO}_3$  doping into  $\gamma$ -glycine improves its hardness.

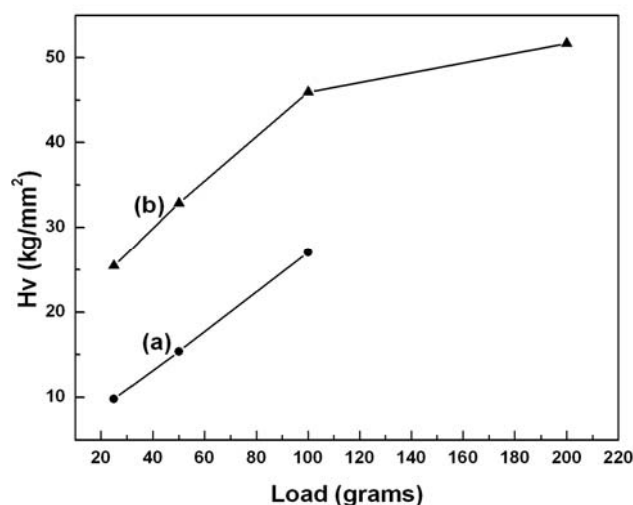


Fig.11 Vickers Hardness of (a)  $\gamma$ -glycine (b)  $\text{AgNO}_3$  doped  $\gamma$ -glycine

#### 4. Conclusions

Optically transparent single crystal of  $\text{AgNO}_3$  doped  $\gamma$ -glycine was conveniently grown by slow-evaporation method. The crystals were transparent and their shape and size were sensitive to the amount of dopant present in the solution during growth. Silver nitrate as a dopant has been found to yield crystals useful for NLO application. Powder XRD, TG-DTA, FTIR and FT-Raman studies confirmed that the  $\text{AgNO}_3$  was doped into  $\gamma$ -glycine. Kurtz powder SHG test confirmed the frequency doubling of the grown crystal and its efficiency was 1.4 times higher than that of KDP. Owing to its wide transparency range, high thermal stability, high hardness value with relatively high SHG efficiency make  $\text{AgNO}_3$  doped  $\gamma$ -glycine a promising material for laser application and fabrication of electro-optic devices.

#### Acknowledgements

One of the authors (R.P) thanks Periyar University for providing University Research Fellowship (URF) and the authors thank Prof. V. Krishnakumar of Periyar University and Dr. A. Thamizhavel of Tata Institute of Fundamental Research for their help in characterization.

#### References

- [1] Yun Zhang, Hua Li, Bin Li, Yunxia Che, Jimin Zheng, Mater. Chem. Phys. **108**, 192 (2008).
- [2] Shankang Gao, Weijun Chen, Guimel Wang, Jianzhong Chen, J. Cryst. Growth **297**, 361

- (2006).
- [3] Tapati Mallik, Tanusree kar, J Cryst. Growth **285**, 178 (2005).
- [4] Xia Yang, Jie Lu, Xiu-Juan Wang, Chi- Bun Ching, J Cryst. Growth **310**, 604 (2008).
- [5] Ambujam K, Selvakumar S, Prem Anand D, Mohamed G, Sagayaraj P, Cryst Res. Technol. **41**,671 (2006).
- [6] M. Narayanan Bhat, S.M. Dharmaprakash, J. Cryst. Growth **242**, 245 (2002).
- [7] Rajul Rajan Choudary, Lata Panicker, R. Chitra, T. Sakuntala, Solid State Commun.**145**,407 (2008).
- [8] Alice Dawson, David R. Allan, Scott A. Belmonte, Stewart J. Clark, William I. F. David, Pamela A. McGregor, Simon Parsons, Colin R. Pulham, Lindsay Sawyer, Cryst Growth Des. **5**, 1415 (2005).
- [9] A.S. Haja Hammed, G. Ravi, R. Jayavel, P. Ramasamy, J Cryst. Growth **250**, 126 (2003).
- [10] P.V. Dhanaraj, N.P. Rajesh NP, Mater. Chem Phys, **115**, 413 (2009).
- [11] K.S. Kunisha, J. Cryst. Growth **23**, 351 (1974).
- [12] Mario T. Rasoda, Maria Leonor, T.S. Duarte, Rui Fausto, Vibration. Spectrosc.**16**, 35 (1998).
- [13] Hans Stenback, J. Raman Spectrosc. **5**, 49 (1976).
- [14] S. K. Kurtz and T.T. Perry, J. Appl. Phys. **39**, 3798 (1968).
- [15] V. Krishnakumar, R. Nagalakshmi, Spectrochim. Acta Part A **68**, 443 (2007).
- [16] T. Kangasekaran, P. Mythili, P. Srinivasan, N. Vijayan, G. Bhagavannarayana, P.K. Kulriya, D. Kanjilal, R. Gopalakrishnan, P. Ramasamy, Cry. Res.Tech. **42**, 1376 (2007).
- [17] K. Meera, S. Aravazhi, P. Santhana, Raghavan, P. Ramasamy, J. Cryst. Growth **211**, 220 (2000).